Nonreciprocal Phonon Laser in an Asymmetric Cavity with an Atomic Ensemble

Kai-Wei Huang(黄凯伟), Xin Wang(王鑫), Qing-Yang Qiu(邱庆洋), Long Wu(吴龙), and Hao Xiong(熊豪)*

School of Physics, Huazhong University of Science and Technology, Wuhan 430074, China

(Received 25 June 2023; accepted manuscript online 7 September 2023)

Phonon lasers, as a novel kind of lasers for generating coherent sound oscillation, has attracted extensive attention. Here, we theoretically propose a nonreciprocal phonon laser in a hybrid optomechanical system, which is composed of an asymmetric Fabry–Pérot cavity, an ensemble of N identical two-level atoms, and a mechanical oscillator. The effective driving amplitude related to driving direction leads to an obvious difference in mechanical gain and threshold power, bringing about a nonreciprocal phonon laser. In addition, the dependence of the phonon laser on the atomic parameters is also discussed, including the decay rate of the atoms and the coupling strength between the atoms and the cavity field, which provides an additional degree of freedom to control the phonon laser action. Our work provides a path to realizing a phonon laser in an atoms-cavity optomechanical system and may aid the manufacture of directional coherent phonon sources.

DOI: 10.1088/0256-307X/40/10/104201

A Fabry–Pérot cavity is composed of two fixed mirrors at both ends of the cavity, which can capture light to enhance the light-matter interaction. Generally, a movable mirror (i.e., cantilever tip)[1,2] is introduced into the cavity to resonate as a harmonic near the balance position,[3] realizing the interaction between light and matter.[4] Due to its great application potential in cooling of mechanical oscillators,[5–7] highly sensitive measurements,[8–12] and gravitational wave detectors,[13,14] this setup, cavity optomechanics (COM),[15,16] has aroused great interests in recent years. This novel mechanism enriches the control methods of photons, and allows the investigation of some fascinating phenomena in the classical and quantum regimes,[17–27] such as optomechanically induced transparency, high-order sideband generation, photon blockade, and entanglement. Further, phonon lasers have been studied experimentally and theoretically[28–33] by manipulating phonons in COM systems. Compared to optical lasers, a phonon laser[34] has the following advantages: the phonon cavity is easy to tune, the speed of a sound wave is significantly slower than that of light, and the phonon is not affected by radiation loss in a vacuum. Thus, phonon lasers can achieve high energy concentration, and perform high-precision non-destructive measurements. In addition, the scheme of phonon lasers can also be achieved in a quantum-dot system.[35,36] A phonon laser generating a coherent phonon source provides an important platform in functional phononic devices[37] and quantum acoustics.[38–40]

In parallel, the nonreciprocal devices that break the physical symmetry enable light to propagate from one direction rather than the other, which plays an extremely important role in wide applications of circulators,[41,42] optical isolators,[43,44] and metamaterials.[45,46] Traditional nonreciprocal devices based on the magneto-optical Faraday effect[47] not only need strong magnetic field and bulky materials, but are also difficult for on-chip integration. In order to overcome these shortcomings, various schemes of nonreciprocal optical devices have been implemented in non-Hermitian systems[48,49] and Kerr resonators,[50,51] as well as time modulation for photonic systems.[52] In particular, many nonreciprocal phenomena have been reported in spinning resonators based on the Sagnac effect,[22,53–57] such as photon blockade, phonon lasers, entanglement, chaos, and sideband responses. Specifically, by coupling atoms with an asymmetric cavity field, optical nonreciprocity transmission has been demonstrated.[58–60] However, as far as we know, the nonreciprocal phonon laser in an asymmetric cavity is rarely considered and remains to be investigated.

Inspired by the advantages of the asymmetric cavity system, we study a hybrid COM system, in which our system is composed of an asymmetric Fabry–Pérot cavity, a two-level atomic ensemble, and a mechanical oscillator to realize a nonreciprocal phonon laser. The hybrid COM system offers the phonon analogue of a two-level laser through phonon mediated optical transitions. Then, the optical inversion generates coherent mechanical gain at the breathing mode, resulting in a phonon laser above the threshold power $P_{\rm th}$.[28] The gain factor of the phonon laser increases from one driving direction and suppresses from the opposite driving direction. The fundamental reason for this is that the attenuations of the asymmetric cavity walls are different, resulting in different driving amplitudes at the same driving power. We find that the isolation parameter linearly changes with the attenuation of the cavity walls and can reach about 24.2 dB. In addition, we introduce an ensemble of atoms to replace one of the cavities in the previously studied phonon laser system,[28,29,54] which provides a new method for controlling the phonon

*Corresponding author. Email: haoxiong1217@gmail.com
© 2023 Chinese Physical Society and IOP Publishing Ltd

laser. Compared to the previous scheme in a spinning resonator,[54] our system is more robust, since it does not need to maintain constant rotational speed and to consider additional rotational kinetic energy. Here, our results provide a method to adjust the phonon laser by the driving direction and the atomic parameters, and offers a guideline for further experiments. Our scheme may provide applications for the atoms-COM system in quantum information processing and nonreciprocal devices.

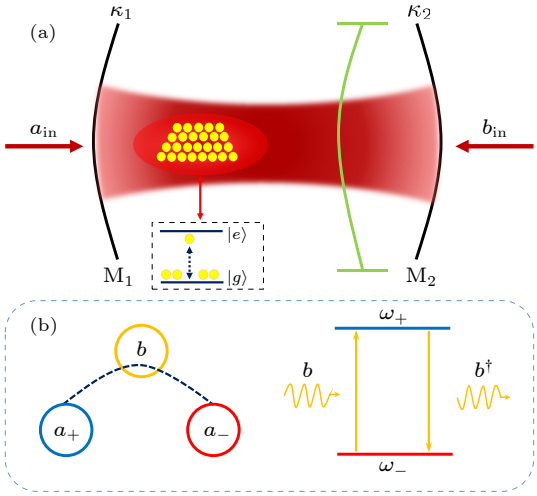

Fig. 1. (a) A schematic diagram of our hybrid optomechanical system. The asymmetric Fabry–Pérot cavity contains an ensemble of N identical two-level atoms and a movable membrane, in which the atoms and the mechanical oscillators interact with cavity modes. Here cavity decay rate κ_1 (κ_2) denotes the loss of cavity mode via M_1 (M_2); $a_{\rm in}$ ($b_{\rm in}$) is forward (backward) input with the same power. Levels $|g\rangle$ and $|e\rangle$ represent the ground and excited states of the atom. (b) Scheme depicting the corresponding optical supermodes coupled by a phonon, as well as the equivalent two-level phonon laser energy-level diagram.

As shown in Fig. 1(a), we present a hybrid optomechanical system including the asymmetrical Fabry–Pérot cavity, the membrane, and the two-level atoms. A movable membrane is regarded as a quantum mechanical harmonic oscillator with frequency $\omega_{\rm m}$ and interacts with the cavity field through the radiation pressure. The two-level atomic ensemble with frequency $\omega_{\rm a}$ is confined by the magneto-optical trap in the cavity and couples to the cavity mode via the dipole interaction.[59] Such a setup of our system can be realized in a SiN membrane on a silicon chip containing a ^{87}Rb atom vapor with buffer gas.[61,62] The cavity mode with frequency $\omega_{\rm c}$ is driven by the pump field with frequency $\omega_{\rm L}$. The cavity decay rates κ_1 and κ_2 of the cavity walls M_1 and M_2 meet the conditions $\kappa_i = -c\cdot\ln(R_i/2L)$, where R_i is the reflectivity of cavity wall M_i ($i = 1, 2$), L is the effective length of the optical cavity, and c is the speed of light in vacuum.[59,60] Generally, the decay rates κ_1 and κ_2 of the cavity walls are unequal, thus breaking the spatial symmetry. Only when $\kappa_1 = \kappa_2 = \kappa_0$, the cavity symmetry is satisfied, where $\kappa_0 = (\kappa_1+\kappa_2)/2$ is defined as the average loss rate of the cavity. The total decay of the cavity is $\kappa_{\rm c} = \kappa_1+\kappa_2+\kappa_{\rm loss}$, where the remaining dissipation rate of the cavity mode $\kappa_{\rm loss}$ can be neglected in the high-quality cavity ($\kappa_{\rm loss}/\kappa_{\rm c} \ll 1$).

Then, the Hamiltonian of our system can be written as ($\hbar = 1$)

$$\begin{aligned} H &= H_0 + H_{\rm int} + H_{\rm dr},\\ H_0 &= \omega_{\rm c}c^\dagger c + \omega_{\rm m}b^\dagger b + \sum_{i=1}^{N}\omega_{\rm a}\sigma_{\rm ee}^{(i)},\\ H_{\rm int} &= gc^\dagger c(b^\dagger + b) + \lambda\sum_{i=1}^{N}(c\sigma_{\rm eg}^{(i)} + c^\dagger\sigma_{\rm ge}^{(i)}),\\ H_{\rm dr} &= i(\varepsilon_{\rm L}c^\dagger e^{-i\omega_{\rm L}t} - \varepsilon_{\rm L}^* c e^{i\omega_{\rm L}t}). \end{aligned} \tag{1}$$

Here, H_0 is the free Hamiltonian of the system, c ($c^\dagger$) and b ($b^\dagger$) are the annihilation (creation) operators of the photon and phonon, respectively, and the third term represents the population operator of the ith atom. In addition, when $e \neq g$, $\sigma_{\rm eg}^{(i)}$ is the electronic projection operator. $H_{\rm int}$ is the interaction Hamiltonian. The first term describes the optomechanical coupling between the photon and mechanical mode with the coupling strength g. The second term describes the dipole interactions between the photon and two-level atoms with the coupling strength $\lambda = \mu\sqrt{\omega_{\rm c}/2\hbar V\varepsilon_0}$, where μ, V, and ε_0 are the dipole moment, the cavity volume, and the vacuum permittivity, respectively. $H_{\rm dr}$ denotes the driving field, where the effective driving strength is $\varepsilon_{\rm L} = \sqrt{2\kappa_i P_{\rm in}/\hbar\omega_{\rm L}}$ ($i = 0, 1, 2$).[59,60] For a fixed power $P_{\rm in}$, obviously the effective driving strength $\varepsilon_{\rm L}$ depends on the driving direction, as κ_1 and κ_2 are different. As shown in Fig. 1(a), we represent $a_{\rm in}$ as the case of the forward input and $b_{\rm in}$ as the case of backward input. We can acquire the gain factor of the phonon laser in the backward case by replacing κ_2 with κ_1.

When the most atoms are initially prepared in the ground state, we can assume that these atoms exist in the cavity as a whole, which has been proved in previous studies.[63,64] Then, we can define a collective transition operator $a = \lim_{N\to\infty}\sum_{i=1}^{N}(\lambda_i^*/J)|g\rangle_{ii}\langle e|$ fulfilling the bosonic commutation relation $[a, a^\dagger] = 1$, where $J = \lambda\sqrt{N} = \sqrt{\sum_{i=1}^{N}|\lambda_i|^2}$ is the total coupling strength between the atomic ensemble and the cavity field. The coupling parameter J can be enhanced with the increase of atomic number N. In a frame rotating at frequency $\omega_{\rm L}$, the Hamiltonian of the system can be rewritten as

$$\begin{aligned} H =& -\Delta_{\rm c}c^\dagger c - \Delta_{\rm a}a^\dagger a + \omega_{\rm m}b^\dagger b + J(c^\dagger a + ca^\dagger)\\ &+ gc^\dagger c(b^\dagger + b) + i(\varepsilon_{\rm L}c^\dagger - \varepsilon_{\rm L}^* c), \end{aligned} \tag{2}$$

where $\Delta_{\rm c} = \omega_{\rm L} - \omega_{\rm c}$ and $\Delta_{\rm a} = \omega_{\rm L} - \omega_{\rm a}$ are the detunings of the cavity field frequency and the atomic transition frequency, respectively.

The Heisenberg motion equations of this atoms-COM system are

$$\begin{aligned} \dot{c} &= (i\Delta_{\rm c} - \kappa_{\rm c})c - ig(b^\dagger + b)c - iJa + \varepsilon_{\rm L},\\ \dot{a} &= (i\Delta_{\rm a} - \kappa_{\rm a})a - iJc,\\ \dot{b} &= -(i\omega_{\rm m} + \gamma_{\rm b})b - igc^\dagger c, \end{aligned} \tag{3}$$

where $\kappa_{\rm a}$ and $\gamma_{\rm b}$ are the decay rate of the two-level atom and mechanical mode, respectively. The quantum noise term can be safely ignored under strong driving conditions, when we only focus on the average number actions.[65] For convenience, we assume that the atom and photon modes are resonant, that is, $\Delta_{\rm c} = \Delta_{\rm a} = \Delta$. Then we can simply derive the steady-state solutions of this system as

$$\begin{aligned} c_{\rm s} &= \frac{-(i\Delta - \kappa_{\rm a})\varepsilon_{\rm L}}{[i\Delta - ig(b^\dagger + b) - \kappa_{\rm c}](i\Delta - \kappa_{\rm a}) + J^2}, \\ a_{\rm s} &= \frac{-iJ\varepsilon_{\rm L}}{[i\Delta - ig(b^\dagger + b) - \kappa_{\rm c}](i\Delta - \kappa_{\rm a}) + J^2}, \\ b_{\rm s} &= \frac{-ig|c_{\rm s}|^2}{i\omega_{\rm m} + \gamma_{\rm b}}. \end{aligned} \tag{4}$$

Similar to optical lasers, the composite resonator can be used to realize the coherent emission of phonons through the inversion of two supermodes.[28] By introducing supermode operators $a_\pm = (a \pm c)/\sqrt{2}$, the Hamiltonian H in Eq. (2) can be rewritten under the condition of the rotating-wave approximation as

$$\begin{aligned} H =& \omega_+ a_+^\dagger a_+ + \omega_- a_-^\dagger a_- + \omega_{\rm m} b^\dagger b \\ &+ \frac{g}{2}(a_+^\dagger a_- b + a_+ a_-^\dagger b^\dagger) \\ &+ \frac{i}{\sqrt{2}}[\varepsilon_{\rm L}(a_+^\dagger + a_-^\dagger) - {\rm H.c.}], \end{aligned} \tag{5}$$

where the supermode frequencies $\omega_\pm = -\Delta \pm J$. The first interaction term in the Hamiltonian (5) describes the annihilation of a phonon and the optical mode transition from the red supermode to the blue supermode, while the second term describes the opposite process, as shown in Fig. 1(b). This can also be seen as stimulated Brillouin scattering, where a blue supermode is converted into a red supermode and a phonon with energy equal to the difference.

In the supermode picture, the dynamical equations of the system can be obtained as

$$\begin{aligned} \dot{a}_+ &= -(i\omega_+ + \kappa)a_+ - \frac{i}{2}gba_- + \frac{\varepsilon_{\rm L}}{\sqrt{2}}, \\ \dot{a}_- &= -(i\omega_- + \kappa)a_- - \frac{i}{2}gb^\dagger a_+ + \frac{\varepsilon_{\rm L}}{\sqrt{2}}, \\ \dot{b} &= -(i\omega_{\rm m} + \gamma_{\rm b})b - \frac{i}{2}ga_+ a_-^\dagger, \end{aligned} \tag{6}$$

with $\kappa = (\kappa_{\rm c} + \kappa_{\rm a})/2$. We set the ladder operator as $p = a_-^\dagger a_+$ and the population difference $\delta n = a_+^\dagger a_+ - a_-^\dagger a_-$ between the optical supermodes a_+ and a_-. Then, the motion equations of the system are rewritten as

$$\begin{aligned} \dot{b} &= -(i\omega_{\rm m} + \gamma_{\rm b})b - \frac{i}{2}gp, \\ \dot{p} &= -2(\kappa + iJ)p + \frac{i}{2}gb\delta n + \frac{1}{\sqrt{2}}(\varepsilon_{\rm L}^* a_+ + \varepsilon_{\rm L} a_-^\dagger). \end{aligned} \tag{7}$$

Due to the fact that the supermode decay is more rapid than the decay of the mechanical oscillator, i.e., $\kappa \gg \gamma_{\rm b}$, compared with the variation of $a_\pm$ and p, b can be seen as a constant. Thus, the supermode degree of freedom can be adiabatically eliminated. Then, we obtain the steady states of the system as

$$\begin{aligned} a_+ &= \frac{\varepsilon_{\rm L}(2i\omega_- + 2\kappa - igb)}{2\sqrt{2}(\beta - 2i\kappa\Delta)}, \\ a_- &= \frac{\varepsilon_{\rm L}(2i\omega_+ + 2\kappa - igb^\dagger)}{2\sqrt{2}(\beta - 2i\kappa\Delta)}, \\ p &= \frac{igb\delta n + \sqrt{2}(\varepsilon_{\rm L}^* a_+ + \varepsilon_{\rm L} a_-^\dagger)}{2[2(\kappa + iJ) - i\omega_{\rm m}]}, \end{aligned} \tag{8}$$

with $\beta = J^2 - \Delta^2 + \kappa^2 + g^2|b|^2/4$.

The result for b can be found by substituting Eq. (8) into Eq. (7) so that $\dot{b} = (-i\omega_{\rm m} - i\omega_0 + G - \gamma_{\rm b})b + D$, with

$$\begin{aligned} \omega_0 =& \frac{g^2(2\,J - \omega_{\rm m})\delta n}{4(2\,J - \omega_{\rm m})^2 + 16\kappa^2} \\ &+ \frac{g^2|\varepsilon_{\rm L}|^2\kappa^2\Delta}{[(2\,J - \omega_{\rm m})^2 + 4\kappa^2](\beta^2 + 4\Delta^2\kappa^2)}, \\ D =& \frac{(\beta + 2\Delta^2)[2\kappa g(2\,J - \omega_{\rm m}) - 2ig\kappa^2]}{2[(2\,J - \omega_{\rm m})^2 + 4\kappa^2](\beta^2 + 4\Delta^2\kappa^2)}, \end{aligned}$$

and the mechanical gain of the phonon laser is $G = G_1 + G_2$, with

$$\begin{aligned} G_1 &= \frac{g^2\kappa\delta n}{2[4\kappa^2 + (2\,J - \omega_{\rm m})^2]}, \\ G_2 &= \frac{|\varepsilon_{\rm L}|^2 g^2(\omega_{\rm m} - 2\,J)\Delta\kappa}{2(\beta^2 + 4\kappa^2\Delta^2)[4\kappa^2 + (2\,J - \omega_{\rm m})^2]}, \end{aligned} \tag{9}$$

where

$$\delta n \approx \frac{2J\Delta|\varepsilon_{\rm L}|^2}{\beta^2 + 4\kappa^2\Delta^2}.$$

In order to clearly show our work, we define three situations: cases A, B, and C. Cases B and C denote an asymmetric cavity with $\kappa_1 = 1.5\kappa_0$ and $\kappa_2 = 0.5\kappa_0$, corresponding to the forward input case ($a_{\rm in}$) and the backward input case ($b_{\rm in}$), respectively. Case A, independent of the input direction, denotes a symmetrical cavity with $\kappa_1 = \kappa_2 = \kappa_0$. Here, we give the specific parameter values used in this study, $\omega_{\rm m}/2\pi = 20\,{\rm MHz}$, $\gamma_{\rm b} = 100\,{\rm Hz}$, $g = 300\,{\rm Hz}$, $\lambda_{\rm L} = 2\pi c/\omega_{\rm L} = 784.3\,{\rm nm}$, $J/2\pi = 10\,{\rm MHz}$, and $\kappa_{\rm c}/2\pi = \kappa_{\rm a}/2\pi = 2\kappa_0/2\pi = 2\,{\rm MHz}$, which appeared in the previous research.[64,66,67] Note that $Q_{\rm c}$ is generally 10^5–10^{10}, and $Q_{\rm m}$ is generally 10^5–10^6.[16] Specifically, when the length of the cavity and the mass of the mechanical oscillator are $L = 1\,{\rm mm}$ and $m = 10\,{\rm pg}$ respectively, we can obtain that the optomechanical coupling strength is $g = \frac{\omega_{\rm c}}{L}\sqrt{\frac{\hbar}{2m\omega_{\rm m}}} \sim 492\,{\rm Hz}$.

In Fig. 2, we investigate the steady-state populations of intracavity photons $|c_{\rm s}|^2$ as a function of the optical detuning $\Delta/\omega_{\rm m}$. It is obvious that the different driving directions (forward or backward) will lead to different steady-state photon numbers $|c_{\rm s}|^2$. The results show that compared with case A, the photon number of the asymmetric cavity in case B, $|c_{\rm s}|^2$, increases while it decreases in case C. This is due to the larger driving amplitude of case B compared to cases A and C. The radiation pressure is proportional to the intracavity photon numbers. Therefore, we can effectively adjust (increase or decrease) the intensity of optomechanical coupling by tuning the direction of the input light.

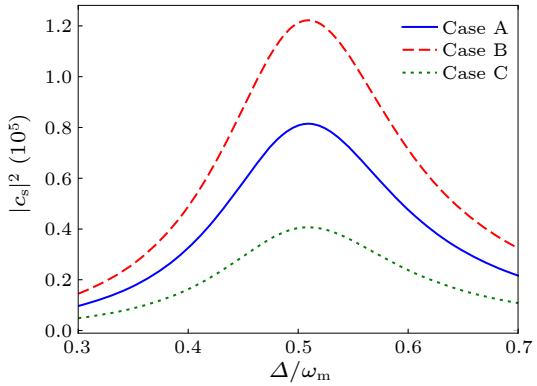

Fig. 2. The steady-state photon number $|c_s|^2$ as a function of the optical detuning Δ/ω_m. The dependence of photon number $|c_s|^2$ on driving direction is obvious, i.e., the forward direction drive (case B) and the backward direction drive (case C) for $\kappa_1 = 1.5\kappa_0$ and $\kappa_2 = 0.5\kappa_0$. Case A ($\kappa_1 = \kappa_2 = \kappa_0$) is a symmetrical cavity. Here, the driving power is $P_{in} = 1\,\mu W$. See text for the other parameters.

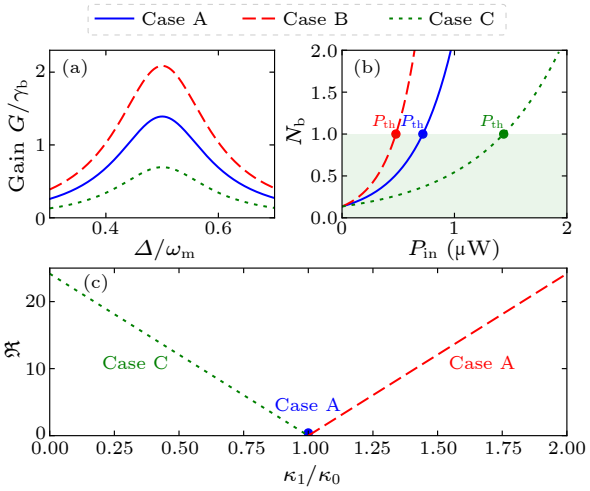

Fig. 3. (a) The mechanical gain G/γ_b as a function of the optical detuning Δ/ω_m in the different cases. The phonon laser can be generated (red dashed curve) or inhibited (green dotted curve) from different input directions. (b) The stimulated emitted phonon number N_b as a function of the pump power P_{in}. The thick points correspond to the threshold power P_{th} at $\Delta/\omega_m = 0.5$, which is determined by the threshold condition $G = \gamma_b$. (c) Dependence of the isolation parameter $\Re$ on the decay rate κ_1. The other parameters are the same as those in Fig. 2.

We present the mechanical gain G as a function of the optical detuning Δ/ω_m for the different cases, as shown in Fig. 3(a). In case A (symmetrical cavity), the gain G of the phonon laser is independent of the driving direction. It is a remarkable fact that only mechanical gain $G > \gamma_b$ makes phonon lasing possible.[28] Since the driving strength is related to the driving direction in an asymmetric cavity, we can enhance the mechanical gain for case B (i.e., $G/\gamma_b > 1$) and apparently suppress it for case C (i.e., $G/\gamma_b < 1$). Therefore, our scheme provides a novel way to control the phonon laser behavior.

With the mechanical gain $G > \gamma_b$ described above, the phonon mode can be amplified. Hence, we calculate the stimulated emitted phonon number N_b, viz.,

$$N_b = \exp[2(G - \gamma_b)/\gamma_b]. \tag{10}$$

According to the threshold condition $G = \gamma_b$, the corresponding threshold pump power P_{th} can be easily deduced as

$$P_{th} = C_i \cdot \frac{[4\kappa^2 + (2J - \omega_m)^2](\beta^2 + 4\kappa^2\Delta^2)}{4J\Delta + 2\Delta(\omega_m - 2J)}, \tag{11}$$

where

$$C_i = \frac{2\hbar\gamma_b\omega_c}{g^2\kappa\kappa_i}, \quad (i = 0, 1, 2).$$

The stimulated emitted phonon number N_b as a function of the driving power P_{in} with $J/2\pi = 10$ MHz and $\Delta/\omega_m = 0.5$ is shown in Fig. 3(b). Intuitively, the higher driving power can generate more phonons. In our scheme, the driving intensity is related to the loss rate of the cavity walls (i.e., M_1 or M_2) in Eq. (11). For the backward drive, the loss rate of the cavity wall is smaller, so a larger input power is needed to achieve a phonon laser. The power thresholds of cases A, B, and C are 0.72 μW, 0.48 μW, and 1.40 μW, respectively. For usable parameters, the power threshold of our results is smaller than the 7 μW reported in experiment and theory.[28,54]

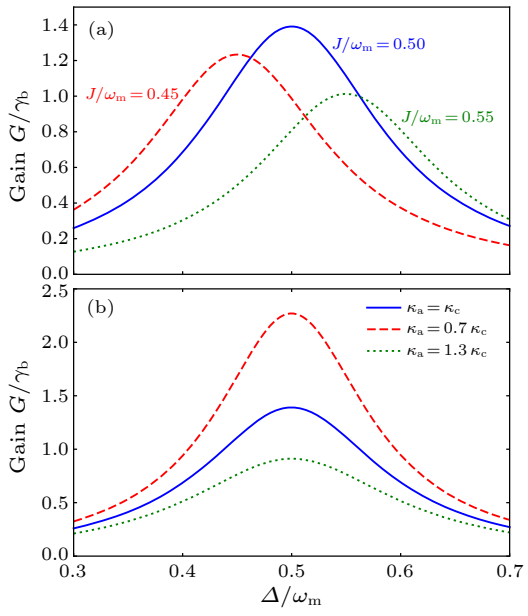

Fig. 4. The mechanical gain G/γ_b of the phonon laser as a function of the optical detuning Δ/ω_m on (a) the atomic coupling strength J and (b) the atomic loss rate κ_a, respectively. The other parameters are the same as those in Fig. 2.

To clearly see the effect of our system on the stimulated emitted phonon, the relationship between κ_1 and κ_2 satisfies $(\kappa_1 + \kappa_2) = 2\kappa_0$, where the average cavity-loss rate $\kappa_0/2\pi = 1$ MHz is fixed. An isolation parameter can be introduced,[68]

$$\Re = 10\left|\log_{10}\frac{N_b(\kappa_1)}{N_b(\kappa_2)}\right|, \tag{12}$$

where nonzero $\Re$ indicates the occurrence of a nonreciprocal phonon laser. The isolation parameter $\Re$ as a function of loss rate of the cavity wall κ_1 for $\Delta/\omega_{\rm m} = 0.5$ is shown in Fig. 3(c). For the phonon laser in a symmetrical cavity (i.e., case A for $\kappa_1 = \kappa_2$), the isolation parameter is $\Re = 0$ (the blue dot), which represents a reciprocal phonon laser. Next, we continue to discuss the asymmetrical cavity case (i.e., $\kappa_1 \neq \kappa_2$), where $\Re \neq 0$ or $N_{\rm b}(\kappa_1) \neq N_{\rm b}(\kappa_2)$ indicates nonreciprocity driven from the two different directions. For convenience, we define $\kappa_1 > \kappa_2$ as the forward input, i.e., case B ($1 < \kappa_1/\kappa_0 < 2$), and vice versa. Obviously, the phonon lasers for both cases (B and C) are dependent on the driving directions, which are indicated by the red dashed curve (for the forward direction) and the green dotted curve (for the backward direction) as shown in Fig. 3(c). The isolation degree of the nonreciprocal phonon laser can be adjusted by changing the loss ratio of the two cavity walls (i.e., M_1 and M_2), and the maximum isolation rate can reach approximately 24.2 dB. Our work makes it easy to turn the phonon laser on or off by adjusting the driving direction due to the asymmetric loss of cavity walls. Meanwhile, this result reveals one of the most important applications of nonreciprocal devices, as a means of protecting lasers from harmful reflections. Apart from that, we calculate the isolation parameter $\Re$ which varies linearly with the decay of the cavity wall (i.e., κ_1 or κ_2) in a robust way. This may provide a way to measure the loss ratio and quality factor of the cavity.

Finally, we study the effect of atomic characteristics on the gain of the phonon laser in the symmetrical cavity (i.e., case A). In Fig. 4, we show the mechanical gain G as a function of the optical detuning $\Delta/\omega_{\rm m}$ for different values of the atomic coupling strength J and the atomic loss rate $\kappa_{\rm a}$. We discuss the gain of the phonon laser in the case of $J/\omega_{\rm m} = 0.45$, 0.50, and 0.55, as shown in Fig. 4(a), in which the atoms-photon coupling strength J can be easily adjusted by the atomic number N. The mechanical gain decreases significantly except for the supermode resonance condition (i.e., $J/\omega_{\rm m} = 0.5$), and the position of the maximum mechanical gain is $\Delta = J$. In the experiment, the decay rate of the two-level atoms $\kappa_{\rm a}$ can be designed. A larger mechanical gain can be realized with smaller $\kappa_{\rm a}$ as shown in Fig. 4(b). It is explained that the smaller atomic dissipation leads to larger photon numbers, which increases the optomechanical coupling between the cavity field and mechanical mode. Importantly, it can be seen from Eq. (9) that the nonreciprocal phonon laser can still be realized, regardless of the atomic situation. This situation is not shown in the text. Our scheme provides a new way to regulate phonon lasers by adjusting the properties of atoms in the atoms-COM systems.

In summary, we have theoretically studied a nonreciprocal phonon laser in a compound optomechanical system, consisting of an asymmetric COM resonator and an ensemble of N two-level atoms. Compared with a symmetrical Fabry–Pérot cavity, the introduction of the asymmetric cavity walls (i.e., M_1 and M_2) significantly changes the steady-state photon number. The mechanical gain of the phonon laser in the asymmetric cavity system depends on the driving direction, making it possible to achieve the nonreciprocal phonon laser. The mechanical gain and the threshold power can be vigorously modulated by adjusting the loss rate κ_1 (or κ_2) of the cavity wall and the driving direction. Then, we also consider the effect of atomic properties on the mechanical gain. These results provide a novel path for manipulating the atoms-COM system through an asymmetric decay of the cavity walls, and may bring about interesting applications in various nonreciprocal devices.

Acknowledgments. This work was supported by the National Key Research and Development Program of China (Grant No. 2021YFA1400700), the National Natural Science Foundation of China (Grant Nos. 11774113 and 12022507), and the Fundamental Research Funds for the Central Universities (Grant No. 2019kfyRCPY111).

References

[1] Metzger C H and Karrai K 2004 *Nature* **432** 1002
[2] Kleckner D and Bouwmeester D 2006 *Nature* **444** 75
[3] Arcizet O, Briant T, Heidmann A, and Pinard M 2006 *Phys. Rev. A* **73** 033819
[4] Ian H, Gong Z R, Liu Y X, Sun C P, and Nori F 2008 *Phys. Rev. A* **78** 013824
[5] Marquardt F, Chen J P, Clerk A A, and Girvin S M 2007 *Phys. Rev. Lett.* **99** 093902
[6] Schliesser A, Rivière R, Anetsberger G, Arcizet O, and Kippenberg T J 2008 *Nat. Phys.* **4** 415
[7] Lai D G, Zou F, Hou B P, Xiao Y F, and Liao J Q 2018 *Phys. Rev. A* **98** 023860
[8] Zhang J Q, Li Y, Feng M, and Xu Y 2012 *Phys. Rev. A* **86** 053806
[9] Xiong H, Si L G, and Wu Y 2017 *Appl. Phys. Lett.* **110** 171102
[10] Xiong H, Liu Z X, and Wu Y 2017 *Opt. Lett.* **42** 3630
[11] Schreppler S, Spethmann N, Brahms N, Botter T, Barrios M, and Stamper-Kurn D M 2014 *Science* **344** 1486
[12] Matsumoto N, Lopez S B C N, Sugawara M, Suzuki S, Abe N, Komori K, Michimura Y, Aso Y, and Edamatsu K 2019 *Phys. Rev. Lett.* **122** 071101
[13] Meers B and MacDonald N 1989 *Phys. Rev. A* **40** 3754
[14] Caves C M 1980 *Phys. Rev. Lett.* **45** 75
[15] Kippenberg T J and Vahala K J 2008 *Science* **321** 1172
[16] Aspelmeyer M, Kippenberg T J, and Marquardt F 2014 *Rev. Mod. Phys.* **86** 1391
[17] Weis S, Rivière R, Deléglise S, Gavartin E, Arcizet O, Schliesser A, and Kippenberg T J 2010 *Science* **330** 1520
[18] Jing H, Özdemir Ş K, Geng Z, Zhang J, Lü X Y, Peng B, Yang L, and Nori F 2015 *Sci. Rep.* **5** 9663
[19] Chembo Y K, Strekalov D V, and Yu N 2010 *Phys. Rev. Lett.* **104** 103902
[20] Xiong H, Si L G, Zheng A S, Yang X, and Wu Y 2012 *Phys. Rev. A* **86** 013815
[21] Rabl P 2011 *Phys. Rev. Lett.* **107** 063601
[22] Huang R, Miranowicz A, Liao J Q, Nori F, and Jing H 2018 *Phys. Rev. Lett.* **121** 153601
[23] Wang K, Wu Q, Yu Y F, and Zhang Z M 2019 *Phys. Rev. A* **100** 053832
[24] Shen S T, Qu Y, Li J H, and Wu Y 2019 *Phys. Rev. A* **100** 023814
[25] Ho M, Oudot E, Bancal J D, and Sangouard N 2018 *Phys. Rev. Lett.* **121** 023602
[26] Hu C S, Yang Z B, Wu H, Li Y, and Zheng S B 2018 *Phys. Rev. A* **98** 023807
[27] Kong C, Liu J, and Xiong H 2023 *Front. Phys.* **18** 12501
[28] Grudinin I S, Lee H, Painter O, and Vahala K J 2010 *Phys. Rev. Lett.* **104** 083901
[29] Jing H, Özdemir S K, Lü X Y, Zhang J, Yang L, and Nori F 2014 *Phys. Rev. Lett.* **113** 053604
[30] He B, Yang L, and Xiao M 2016 *Phys. Rev. A* **94** 031802

[31] Lü H, Özdemir S K, Kuang L M, Nori F, and Jing H 2017 *Phys. Rev. Appl.* **8** 044020
[32] Zhang Y L, Zou C L, Yang C S, Jing H, Dong C H, Guo G C, and Zou X B 2018 *New J. Phys.* **20** 093005
[33] Lin Q, He B, and Xiao M 2021 *Phys. Rev. Res.* **3** L032018
[34] Vahala K, Herrmann M, Knünz S, Batteiger V, Saathoff G, Hänsch T W, and Udem T 2009 *Nat. Phys.* **5** 682
[35] Kabuss J, Carmele A, Brandes T, and Knorr A 2012 *Phys. Rev. Lett.* **109** 054301
[36] Khaetskii A, Golovach V N, Hu X, and Žutić I 2013 *Phys. Rev. Lett.* **111** 186601
[37] Li N B, Ren J, Wang L, Zhang G, Hänggi P, and Li B W 2012 *Rev. Mod. Phys.* **84** 1045
[38] Kemiktarak U, Durand M, Metcalfe M, and Lawall J 2014 *Phys. Rev. Lett.* **113** 030802
[39] Cohen J D, Meenehan S M, MacCabe G S, Gröblacher S, Safavi-Naeini A H, Marsili F, Shaw M D, and Painter O 2015 *Nature* **520** 522
[40] Ganesan A, Do C, and Seshia A 2017 *Phys. Rev. Lett.* **118** 033903
[41] Scheucher M, Hilico A, Will E, Volz J, and Rauschenbeutel A 2016 *Science* **354** 1577
[42] Wang X, Yang W X, Chen A X, Li L, Shui T, Li X, and Wu Z 2022 *Quantum Sci. Technol.* **7** 015025
[43] Fiederling R, Keim M, Reuscher G, Ossau W, Schmidt G, Waag A, and Molenkamp L W 1999 *Nature* **402** 787
[44] Borlenghi S, Wang W, Fangohr H, Bergqvist L, and Delin A 2014 *Phys. Rev. Lett.* **112** 047203
[45] Mahmoud A M, Davoyan A R, and Engheta N 2015 *Nat. Commun.* **6** 8359
[46] Hamann A R, Müller C, Jerger M, Zanner M, Combes J, Pletyukhov M, Weides M, Stace T M, and Fedorov A 2018 *Phys. Rev. Lett.* **121** 123601
[47] Dötsch H, Bahlmann N, Zhuromskyy O, Hammer M, Wilkens L, Gerhardt R, Hertel P, and Popkov A F 2005 *J. Opt. Soc. Am. B* **22** 240
[48] Bender N, Factor S, Bodyfelt J D, Ramezani H, Christodoulides D N, Ellis F M, and Kottos T 2013 *Phys. Rev. Lett.* **110** 234101
[49] Peng B, Özdemir K, Lei F, Monifi F, Gianfreda M, Long G L, Fan S, Nori F, Bender C M, and Yang L 2014 *Nat. Phys.* **10** 394
[50] Del Bino L, Silver J M, Woodley M T M, Stebbings S L, Zhao X, and Del'Haye P 2018 *Optica* **5** 279
[51] Kong C, Xiong H, and Wu Y 2019 *Phys. Rev. Appl.* **12** 034001
[52] Sounas D L and Alú A 2017 *Nat. Photon.* **11** 774
[53] Xue W S, Shen H Z, and Yi X X 2020 *Opt. Lett.* **45** 4424
[54] Jiang Y, Maayani S, Carmon T, Nori F, and Jing H 2018 *Phys. Rev. Appl.* **10** 064037
[55] Jiao Y F, Zhang S D, Zhang Y L, Miranowicz A, Kuang L M, and Jing H 2020 *Phys. Rev. Lett.* **125** 143605
[56] Zhang D W, Zheng L L, You C, Hu C S, Wu Y, and Lü X Y 2021 *Phys. Rev. A* **104** 033522
[57] Wang X, Huang K W, and Xiong H 2023 *Opt. Express* **31** 5492
[58] Xia X W, Xu J P, and Yang Y P 2014 *Phys. Rev. A* **90** 043857
[59] Yang P F, Xia X W, He H, Li S K, Han X, Zhang P, Li G, Zhang P F, Xu J P, Yang Y P, and Zhang T C 2019 *Phys. Rev. Lett.* **123** 233604
[60] Xia X W, Zhang X Q, Xu J P, Li H Z, Fu Z Y, and Yang Y P 2021 *Phys. Rev. A* **104** 063713
[61] Thompson J D, Zwickl B M, Jayich A M, Marquardt F, Girvin S M, and Harris J G E 2008 *Nature* **452** 72
[62] Akulshin A M, Barreiro S, and Lezama A 1998 *Phys. Rev. A* **57** 2996
[63] Gu K H, Yan X B, Zhang Y, Fu C B, Liu Y M, Wang X, and Wu J H 2015 *Opt. Commun.* **338** 569
[64] Liu Z X, Xiong H, and Wu Y 2018 *Phys. Rev. A* **97** 013801
[65] Gardiner C, Zoller P, and Zoller P 2004 *Quantum Noise: A Handbook of Markovian and Non-Markovian Quantum Stochastic Methods with Applications to Quantum Optics* (Berlin: Springer Science & Business Media)
[66] Baumann K, Guerlin C, Brennecke F, and Esslinger T 2010 *Nature* **464** 1301
[67] Jiang Y J, Lv H, and Jing H 2018 *Chin. Phys. Lett.* **35** 044205
[68] Coulais C, Sounas D, and Alù A 2017 *Nature* **542** 461